

# Ising model on a *restricted* scale-free network

R. A. Dumer\* and M. Godoy†

*Instituto de Física - Universidade Federal de Mato Grosso, 78060-900, Cuiabá, Mato Grosso, Brazil.*

The Ising model on a *restricted* scale-free network (SFN) has been studied employing Monte Carlo simulations. This network is described by a power-law degree distribution in the form  $P(k) \sim k^{-\alpha}$ , and is called *restricted*, because independently of the network size, we always have fixed the maximum  $k_m$  and a minimum  $k_0$  degree on distribution, being that for it, we only limit the minimum network size of the system. We calculated the thermodynamic quantities of the system, such as, the magnetization per spin  $m_L$ , the magnetic susceptibility  $\chi_L$ , and the reduced fourth-order Binder cumulant  $U_L$ , as a function of temperature  $T$  for several values of lattice size  $N$  and exponent  $1 \leq \alpha \leq 5$ . For the values of  $\alpha$ , we have obtained the finite critical points due to we also have finite second and fourth moments in the degree distribution, and the phase diagram was constructed for the equilibrium states of the model in the plane  $T$  versus  $k_0$ ,  $k_m$ , and  $\alpha$ , showing a transition between the ferromagnetic  $F$  to paramagnetic  $P$  phases. Using the finite-size scaling (FSS) theory, we also have obtained the critical exponents for the system, and a mean-field critical behavior is observed.

## I. INTRODUCTION

Hyperlinks pointing from one web page to another (World Wide Web), computers physically linked (internet), actors that have acted in a movie together, scientists that have an article together, and proteins that bind together experimentally, are some of the cases that, when analyzed in terms of nodes and edges of a network, they are part of a broad group of real systems in which the degree distribution has a power-law tail [1, 2]. This degree distribution has the form  $P(k) \sim k^{-\alpha}$ , representing the probability of a site in the network to have a degree  $k$ , i.e.,  $k$  edges linked to it, with exponent  $\alpha$ . Barabási-Albert [3] proposed a growing process of network creation, in which the degree distribution resultant also has the form of power-law. That growing process is based only on two generic mechanisms: (i) networks expand continuously by the addition of new vertices, and (ii) new vertices attach preferentially to sites that are already well connected. With these mechanisms, most connected sites are most likely to receive new connections, and a “rich-get-richer”, and self-organization phenomenon, as in real networks, is observed.

Due to the applicability of the networks with a power-law degree distribution, also called scale-free networks, it was been implemented in many physical problems [4–11]. Highlighting the critical phenomena arising from the Ising model, from an analytical way, Dorogovtsev, Goltsev, and Mendes showed that its critical behavior is very dependent on the distribution of connections [12, 13]. From this dependence, when  $\alpha > 5$  in  $P(k)$ , its fourth moment  $\langle k^4 \rangle$  is convergent and a mean-field critical behavior is obtained. When,  $3 < \alpha \leq 5$ , anomalous behavior of the thermodynamics quantities is observed, due to divergence in  $\langle k^4 \rangle$ , but when  $\alpha \leq 3$ , the divergence is in the second moment,  $\langle k^2 \rangle$ , and the criticality vary with the size of the system, being an infinity order phase transition in the thermodynamic limit. In the network proposed in the Barabási-Albert (BA) model [3], the exponent is limited by  $\alpha = 3$ , and in previews of approximate and numerical results, the infinity order phase transition is verified [14, 15]. In addition to  $\alpha = 3$ , the cases where  $\langle k^4 \rangle$  and  $\langle k^2 \rangle$  are convergent and divergent, by Monte Carlo simulations [16] and replica method [17], have been proven the non-trivial critical exponents, beyond the and size-dependent critical temperature.

In these Monte Carlo simulations, the SFN, constructed with a selected value of  $\alpha$ , is absent from the two growing mechanisms in the BA model and created distributing degrees for the vertices based on the exact value of  $P(k) = Ak^{-\alpha}$  [16]. For this exact value is predefined the minimum  $k_0$  and maximum  $k_m$  degrees of the network, and calculated the normalization constant of the distribution,  $A = \sum_{k=k_0}^{k_m} k^\alpha$ . In this sense, supposing that the number of sites with the degree  $k_m$  is  $N_{k_m} = 1$ , the network size with these characteristics is given by  $N = k_m^\alpha / A$ . From this way, fixing  $k_0$  and varying the network sizes  $N$ , Herrero [16] could reproduce the main critical phenomena seen analytically [12, 13], by the FSS analysis of networks with also non-fixed  $k_m$ .

In this work, we investigated the Ising model on a *restricted* SFN, where each site of the network is occupied by a spin variable  $\sigma = 1/2$  that can assume values  $\pm 1$ . Our network was built for various integer values of the exponent  $\alpha$ , and divided into two sublattices, each connection distributed by  $P(k)$ , a power-law degree distribution, which should

---

\* rafaeldumer@fisica.ufmt.br

† mgodoy@fisica.ufmt.br

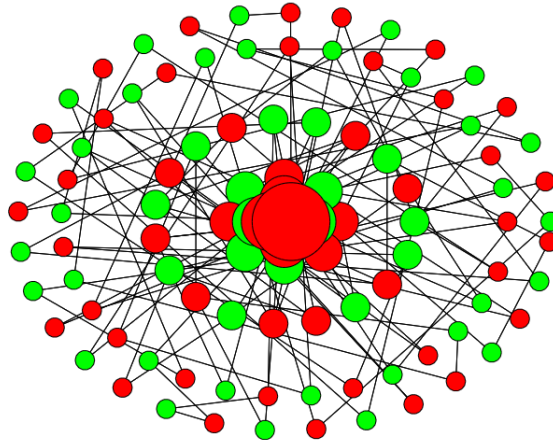


Figure 1. Schematic representation of the *restricted* SFN. The red circles indicate the sites on one of the sublattices, the green circles are the sites on the other sublattice, and the black solid lines are the connections between the two sublattices. The size of the circles is proportional to the sites degree, varying from  $k_0 = 2$  to  $k_m = 8$ , with  $\alpha = 3$ , and  $N = 10^2$ .

connect these sublattices. Besides that, in a similar way to what was proposed by Herrero [16] to construct its random uncorrelated network, we also preview define who will be  $k_0$  and  $k_m$  in our system. These values are kept fixed while we vary the size  $N$  of the network. Thereunto, the minimal network size that we can use is defined by  $N_0 = k_m^\alpha / A$  and is not always obtained  $N_{k_m} = 1$ . However, as we have the same degrees on all network sizes, we always have a convergent  $\langle k^2 \rangle$  and  $\langle k^4 \rangle$ , and consequently finite transitions point, for ferromagnetic to paramagnetic phases, in the whole values of  $\alpha$ . Thus here, through Monte Carlo simulations, we have built phases diagrams of critical temperature  $T_c$  as a function of  $k_0$  and  $k_m$  for the studied values of  $\alpha$ , and using the FSS theory, we have obtained the critical exponents for the system.

This article is organized as follows: In Section II, we describe the network used and the Hamiltonian model of the system. In Section III, we present the Monte Carlo simulation method, some details concerning the simulation procedures and the thermodynamic quantities of the system also necessary for the application of FSS analysis. The behavior of thermodynamic quantities, phases diagrams, and critical exponents are described in Section IV. Finally, in Section V, we present our conclusions.

## II. MODEL

The Ising model studied in this work have  $N = L^2$  spins  $\sigma_i = \pm 1$ , on a *restricted* SFN and a ferromagnetic interaction of strength  $J_{ik}$ . To distribute the connections on this network, we first defined  $k_0$ ,  $k_m$  and  $\alpha$ , i.e., the minimum and maximum degree that the network is required to have and its exponent on the distribution, respectively. Next, we calculated the normalization constant of the distribution,  $A = \sum_{k=k_0}^{k_m} k^\alpha$ , and found the smallest network that we will use in the system,  $N_0 = k_m^\alpha / A$ . With these values, we create a set of site numbers,  $\{N_k\}$ , that will have the respective degrees  $k$ ,  $N_k = AN/k^\alpha$ , and distribute them by the network. For this distribution of connections, we have divided the network into two sublattices, where one sublattice plays the role of central spins, while the other sublattice contains the spins in which the central spins can connect. Thus, starting with the lowest degree, we select one site  $i$  on the network, and its sublattice will be the sublattice of central spins, then, from the other sublattice, we select one site  $j$  at random, that has not yet received their respective connections. With this, we couple  $j$  to the neighbors of  $i$ , and for the site  $j$  we couple the site  $i$  to their neighbors. This process is done until  $i$  has their  $k$  connections and visited all the set  $\{N_k\}$ . It is valid to say that, for this network, there is not need to create these sublattices and the connections can be created completely randomly between free sites, but here, this implementation was done as a way to prepare the system for future works in non-equilibrium systems without loss of generality.

In Fig. 1, we displayed an example of the network, with  $\alpha = 3$ ,  $k_0 = 2$ ,  $k_m = 8$  and  $N = 10^2$ . The sites in the middle of the figure are the more connected, while the peripheral sites are the less connected, and sites from the sublattice green are only connected with sites from the sublattice red.

Based on this construction, throughout work, we have selected the integer values of  $1 \leq \alpha \leq 5$ , and network sizes

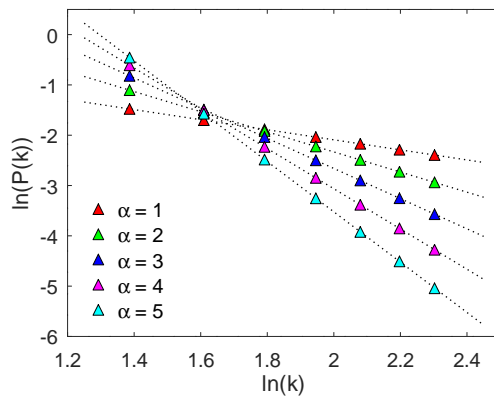


Figure 2. Log-log plot of the degree distribution on *restricted* SFN for some selected values of  $\alpha$ , as shown in the figure. All curves refer to the network size  $N = 256^2$ , minimum degree  $k_0 = 4$  and maximum degree  $k_m = 10$ . The dotted lines have the exact expected slopes,  $\alpha$ , and the errors of the slopes are in order of  $10^{-4}$  and the error bars are the same size or smaller than the symbols.

$(32)^2 \leq N \leq (256)^2$  to study the Ising model. In Fig. 2, we shown the degree distribution in the largest network size of the system for these selected values of  $\alpha$ . With these distributions in the log-log plot, we can see that the construction method used here, guarantees the power-law form, as predicted in SFN.

The ferromagnetic Ising spin energy is described by the Hamiltonian on the form

$$\mathcal{H} = - \sum_{\langle i,j \rangle} J_{ij} \sigma_i \sigma_j \quad (1)$$

where the sum is over all pair of spins, and  $J_{ij}$  is the ferromagnetic interaction, and assuming the value of unity if sites  $i$  and  $j$  are connected by a link.

### III. MONTE CARLO SIMULATIONS

In the simulation of the system specified by the Hamiltonian in Eq. (1) and with a *restricted* SFN, we have chosen the initial state of the system with all spins in the random states, and a new configuration is generated by a Markov process. In this process, for a given temperature  $T$ , exponents  $\alpha$  of the degree distribution, network size  $N$ , and minimum  $k_0$  and maximum  $k_m$  degree, we choose at random a spin  $\sigma_i$  on the network and change its state by the one-spin flip mechanism with a transition rate given by the following Metropolis prescription

$$W(\sigma_i \rightarrow \sigma'_i) = \begin{cases} e^{(-\Delta E/k_B T)} & \text{if } \Delta E > 0 \\ 1 & \text{if } \Delta E \leq 0 \end{cases}, \quad (2)$$

where  $\Delta E$  is the change in energy after flipping the spin,  $\sigma_i \rightarrow \sigma'_i$ ,  $k_B$  is the Boltzmann constant, and  $T$  the temperature of the system. Therefore, in this scenario, the acceptance of a new state is made if  $\Delta E \leq 0$ , but, in the case where  $\Delta E > 0$ , the acceptance is pondered by the probability  $\exp(-\Delta E/k_B T)$  and just it is accepted by choosing a random number  $0 < \xi < 1$ , where  $\xi \leq \exp(-\Delta E/k_B T)$ . On the other hand, if no one of these conditions was satisfied, we do not change the state of the spin.

Repeating the Markov process  $N$  times, we have a Monte Carlo Step (MCS). In our simulations, we have waited  $10^4$  MCS for the system reach the equilibrium state, in all lattice sizes and value of the parameters. To calculate the thermal averages of the interest quantities, we used more  $4 \times 10^4$  MCS. The average over samples were done using 10 independent samples for any configuration.

After reaching the equilibrium state, we have measured the following thermodynamic quantities: magnetization per spin  $m_L$ , magnetic susceptibility  $\chi_L$  and reduced fourth-order Binder cumulant  $U_L$ :

$$m_L = \frac{1}{N} \left[ \left\langle \sum_{i=1}^N \sigma_i \right\rangle \right], \quad (3)$$

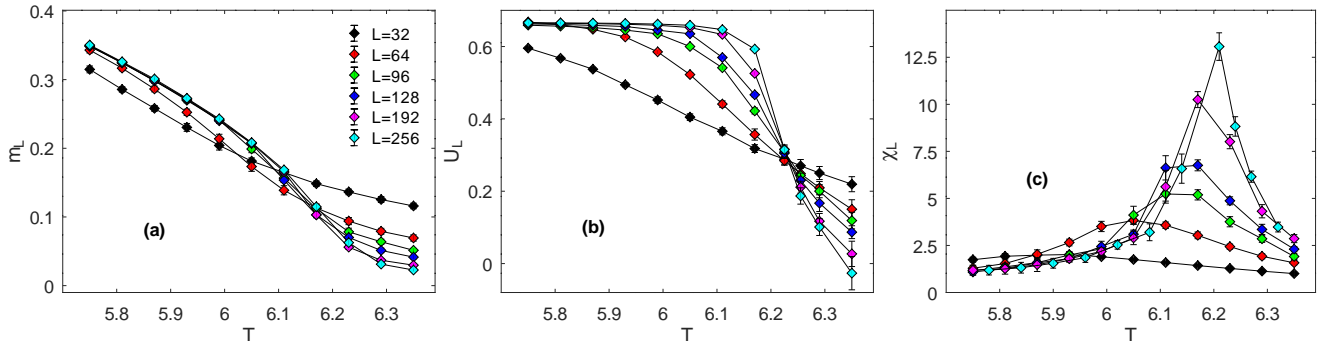


Figure 3. Thermodynamic quantities as a function of temperature  $T$  for a fixed value of  $\alpha = 1$ ,  $k_0 = 4$  and  $k_m = 10$ , and for different network sizes, as present in the figure. (a) Magnetization  $m_L$ , (b) reduced fourth-order Binder cumulant  $U_L$ , and (c) susceptibility  $\chi_L$ .

$$\chi_L = \frac{N}{k_B T} \left[ \langle m_L^2 \rangle - \langle m_L \rangle^2 \right], \quad (4)$$

$$U_L = 1 - \frac{\langle m_L^4 \rangle}{3 \langle m_L^2 \rangle^2}, \quad (5)$$

where  $[\dots]$  represents the average over the samples, and  $\langle \dots \rangle$  the thermal average over the MCS in the equilibrium state. In the vicinity of the critical temperature  $T_c$ , the above-defined quantities obey the following finite-size scaling relations:

$$m_L = L^{-\beta/\nu} m_0(L^{1/\nu} \epsilon), \quad (6)$$

$$\chi_L = L^{\gamma/\nu} \chi_0(L^{1/\nu} \epsilon), \quad (7)$$

$$U'_L = L^{1/\nu} \frac{U'_0(L^{1/\nu} \epsilon)}{T_c}, \quad (8)$$

where  $\epsilon = (T - T_c)/T_c$ ,  $m_0(L^{1/\nu} \epsilon)$ ,  $\chi_0(L^{1/\nu} \epsilon)$  and  $U'_0(L^{1/\nu} \epsilon)$  are the scaling functions, and  $\beta$ ,  $\gamma$  and  $\nu$  are the magnetization, magnetic susceptibility and length correlation critical exponents, respectively.

Using the Eqs. (6), (7), (8) and the data from simulations for the network sizes  $32 \leq L \leq 256$ , we have obtained the critical exponents ratios,  $\beta/\nu$ ,  $\gamma/\nu$  and  $1/\nu$  from the slope of  $m_L(T_c)$ ,  $\chi_L(T_c)$  and  $U'_L(T_c)$  as a function of  $L$  in a log-log plot. Aside from that, we also used data collapse from scaling functions to estimate the critical exponent values.

#### IV. RESULTS

The interesting results about the critical phenomena in complex networks, more specifically on random uncorrelated networks, led us to understand the importance of its degree distribution and respective moments. The Ising model on the uncorrelated SFN, in the limit where  $N \rightarrow \infty$ ,  $k_m \rightarrow \infty$  and the changing in its structure for  $\alpha > 3$ , decreases the number of more connected spins, admitting a finite-order phase transition until reaches the standard mean-field critical behavior due to strong correlations of most connected vertices in their neighborhood [12, 13]. However, here, by the restriction of maximum  $k_m$  and minimum  $k_0$  degree, and minimum network size, when  $N \rightarrow \infty$ ,  $k_m$  keeps finite, consequently changing the number of more and less connected sites, their correlations, and the critical phenomena as we can see in our results.

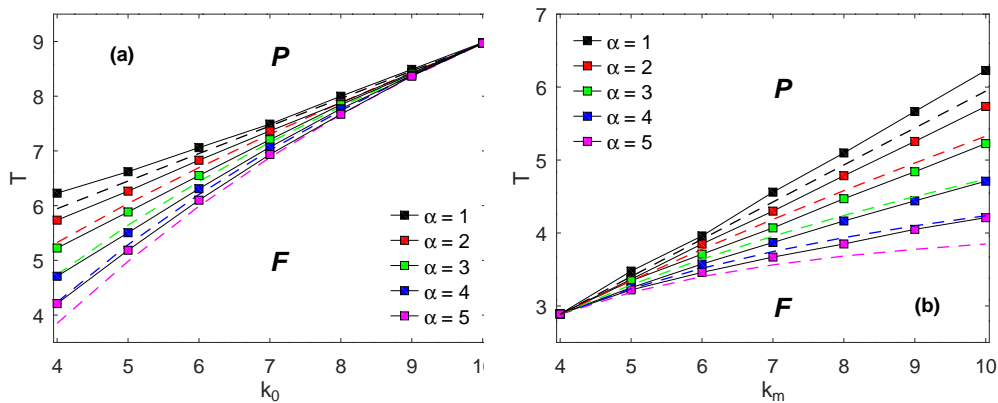


Figure 4. (a) Phase diagram of temperature  $T$  as a function of  $k_0$  for a fixed value of  $k_m = 10$  and (b) as a function of  $k_m$  for a fixed value of  $k_0 = 4$ . Both figures representing transitions from  $F$  to  $P$  phases. The solid lines are just guide for the eyes and the dashed lines represent the analytical result obtained by Eq. (9).

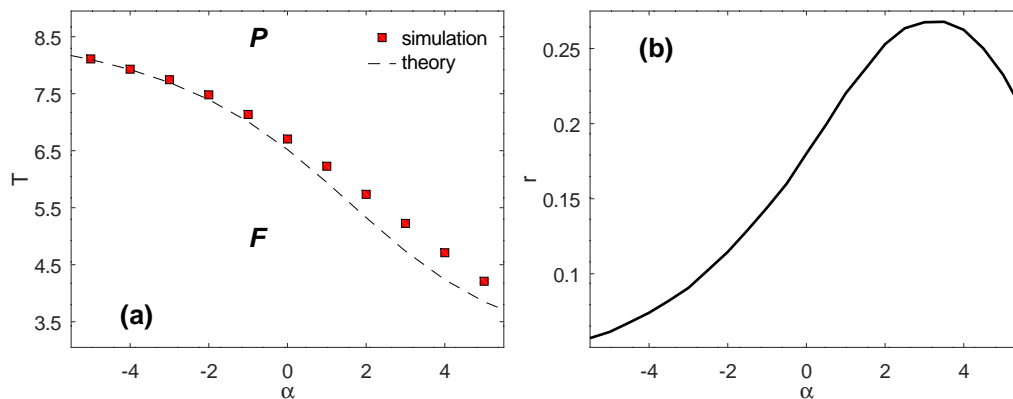


Figure 5. (a) Phase diagram of temperature  $T$  as a function of  $\alpha$ , for the transition between  $F$  to  $P$  phases, with fixed values of  $k_0 = 4$  and  $k_m = 10$ . The dashed line is the theoretical result expected for random uncorrelated networks and obtained using the Eq. (9). The red squares are the simulation data points on the *restricted* SFN, and calculated by the crossing of  $U_L$  curves. (b) Degree-degree correlations  $L$  as a function of  $\alpha$  and obtained by the Eq. 10.

To begin with, we have identified the point of transition between the ferromagnetic  $F$  to the paramagnetic  $P$  phases through the curves of the fourth-order Binder cumulant  $U_L$  with different network sizes [18–21]. This critical point and second-order phase transition can be identified by the crossing point of  $U_L$  curves, and an example is shown in Fig. 3. In this figure, we have presented as one of the best results for thermodynamic quantities obtained by Eqs. (3), (4) and (5), being that in Fig. 3(a), we can see the behavior of the magnetization  $m_L$  as a function of  $T$ , the reduced fourth-order Binder cumulant  $U_L$  (see Fig. 3(b)), and the magnetic susceptibility  $\chi_L$  (see Fig. 3(c)). In this case, we have used a fixed value of  $\alpha = 1$ ,  $k_0 = 4$  and  $k_m = 10$ , and different network sizes, as present in Fig. 3.

With the critical points obtained, the phase diagrams were built, see Fig. 4. For these diagrams, the temperature as a function of  $k_0$ ,  $k_m$  and  $\alpha$  is studied, and for that, we have used  $4 \leq k_0, k_m \leq 10$  and integer values of  $\alpha$ . The continuous transition lines can be seen in Fig. 4(a) for temperature  $T$  versus  $k_0$ , and for a fixed value of  $k_m = 10$ , and some selected values of  $\alpha$ , where we can verify that have a finite critical point for all the values of  $\alpha$ . Because we have a fixed value of  $k_m$ , as we increase  $k_0$  the number of different degrees on the network decrease until the whole system has the coordination number  $k_0 = k_m = 10$ , and when that happens, the exponent of the degree distribution is no longer important, returning us to a unique critical point for all the exponents  $\alpha$ . On the other hand, in the case where  $k_0 \neq k_m$ , the degrees can be distributed on the network, and for different values of  $\alpha$  is showed the presence of different critical points in the system, being that each value of  $\alpha$  is responsible for a distinct curve in Fig. 4(a). Instead, we can fix  $k_0 = 4$  and varying  $k_m$ , and as can be seen in Fig. 4(b) for  $T$  versus  $k_m$ . Thus, we can observe the presence of the same qualitative behavior, like, continuous transitions lines for the whole parameter values, distinct curves for distinct exponents  $\alpha$ , and a unique critical point when  $k_m = k_0$ . Despite these similarities, if we approximate these curves by a linear fit, the slopes of curves in Fig. 4(a) have an increasing behavior according we increase  $\alpha$ , while the slopes of curves in Fig. 4(b) decrease according to increase  $\alpha$ . This is visually perceptible, but also is explicit in the

$\alpha$	$\Theta_{k_0}$	$\Theta_{k_m}$	$-\beta/\nu$	$\gamma/\nu$	$1/\nu$
1	$0.46 \pm 0.04$	$0.55 \pm 0.04$	$0.45 \pm 0.04$	$1.04 \pm 0.05$	$0.99 \pm 0.05$
2	$0.54 \pm 0.02$	$0.47 \pm 0.01$	$0.53 \pm 0.04$	$0.92 \pm 0.06$	$0.95 \pm 0.04$
3	$0.62 \pm 0.04$	$0.38 \pm 0.03$	$0.52 \pm 0.04$	$0.91 \pm 0.05$	$0.97 \pm 0.06$
4	$0.71 \pm 0.05$	$0.30 \pm 0.03$	$0.51 \pm 0.06$	$0.90 \pm 0.07$	$0.96 \pm 0.05$
5	$0.79 \pm 0.08$	$0.21 \pm 0.06$	$0.52 \pm 0.07$	$0.90 \pm 0.08$	$0.95 \pm 0.04$

Table I. Slopes of curves presented in Fig. 4(a),  $\Theta_{k_0}$ , and Fig. 4(b),  $\Theta_{k_m}$ , and the ratio between the critical exponents obtained by the method presented in Fig. 6.

variables  $\Theta_{k_0}$  and  $\Theta_{k_m}$  presented in Tab. I.

When  $\alpha > 3$ , the analytical calculations predict well-defined finite critical points in the  $F$  to  $P$  phase transition [12, 13, 17]. As a matter of comparison, the analytical results for the random uncorrelated networks in which is known its first and second moment of degree distribution, and introduced by equation

$$T_c = \frac{2}{\ln\left(\frac{\langle k^2 \rangle}{\langle k \rangle^2 - 2\langle k \rangle}\right)}, \quad (9)$$

also were plotted in Fig. 4 (see dashed lines). As we can see in this figure, we also have plotted values of  $\alpha < 3$ , and its possible because instead of the usual integral approximation of the sum in  $\langle k \rangle$  and  $\langle k^2 \rangle$ , where result in  $T_c \rightarrow 0$  and  $T_c \rightarrow \infty$ , with  $\alpha = 2$  and  $\alpha = 3$ , respectively, we have kept the sum, once that  $k_0$  and  $k_m$  are restricted. The dashed lines on Figs. 4(a) and 4(b) are described by Eq. (9), and apparently, we can observe the same signature, both in the analytical result and simulations. However, in the building process of our *restricted* SFN, more connected sites are the last to be chosen to add their connections, and their missing connections only can be attached to sites that were not chosen yet, i.e., we have implicitly an increase of the degree-degree correlations [22, 23], once in the last steps of building the network, more connected sites only can connect with more connected sites. These correlations can be identified in the higher values of  $T_c$  in the simulations if compared with analytical results, because as we increase the difference between  $k_0$  and  $k_m$ , we also increase the number of different degrees on the network and consequently increase the possibility of degree-degree correlations.

The degree-degree correlations were calculated here using the equation

$$r = \frac{M^{-1} \sum_i u_i v_i - [M^{-1} \sum_i \frac{1}{2} (u_i + v_i)]^2}{M^{-1} \sum_i \frac{1}{2} (u_i^2 + v_i^2) - [M^{-1} \sum_i \frac{1}{2} (u_i + v_i)]^2}, \quad (10)$$

for a network with  $M$  edges connecting the pair of vertices, and their respective  $u_i$  and  $v_i$  degrees, as defined in Ref. [22]. These correlations are shown in Fig. 5(b) as a function of  $\alpha$ , and besides being independent of network size, have a descending behavior according the number of more connected sites increase, and ascending when this number become small, but relevant yet. The peak of the correlation  $r$  was observed in  $\alpha = 3.5$  and has value  $r = 0.268$ . Therefore, the network presents a associative mixing, confirming that sites with high degree, on the network, prefers to connect on more connected sites, which is the case for high values of  $\alpha$ . It is interesting to mention that many social networks also have significant associative mixing, and do not present some in complex network models, like random graphs or growing network model (BA model [22]).

Now that we have established the critical behavior of the system as a function of the degrees on the network, using the most distinct and distributed values of degree,  $k_0 = 4$  and  $k_m = 10$ , we will effectively verify the critical behavior of the *restricted* SFN as a function of  $\alpha$ . As presented in Fig. 5(a), this verification was first done by using some points in Fig. 4 by simulation data, and Eq. (9). By Eq. (9) is explicit the lower values of  $T_c$  where we have a high degree-degree correlation, but, for small  $r$ , i.e., in lower values of  $\alpha$ , the simulation results approach to analytical result of a random uncorrelated network. That approach to analytical results is also resultant of small influence of more connected sites, and also observed for  $\alpha > 3.5$ . By the fixed values of  $k_m$  and  $k_0$ , the minimum and maximum critical temperature values is limited to the case where  $k_m = k_0 = 4$  on Fig. 4(b) as we increase  $\alpha$ , because we will never reach a network with coordination number 4, without losing the structure of degrees. The same is observable decreasing  $\alpha$ , because we have the limit of  $T_c$ , in the case  $k_m = k_0 = 10$  present in Fig. 4 (a) and unreachable in our *restricted* SFN. For some critical points in Fig. 5,  $1 \leq \alpha \leq 5$ , we have its explicit estimation and respective errors presented in Tab. II.

Analytical results for the random uncorrelated networks also extend to critical exponents in the Ising model, being that is predicted for magnetic critical exponent, a mean-field character,  $\beta = 1/2$  for  $\alpha > 5$ , with logarithmic corrections

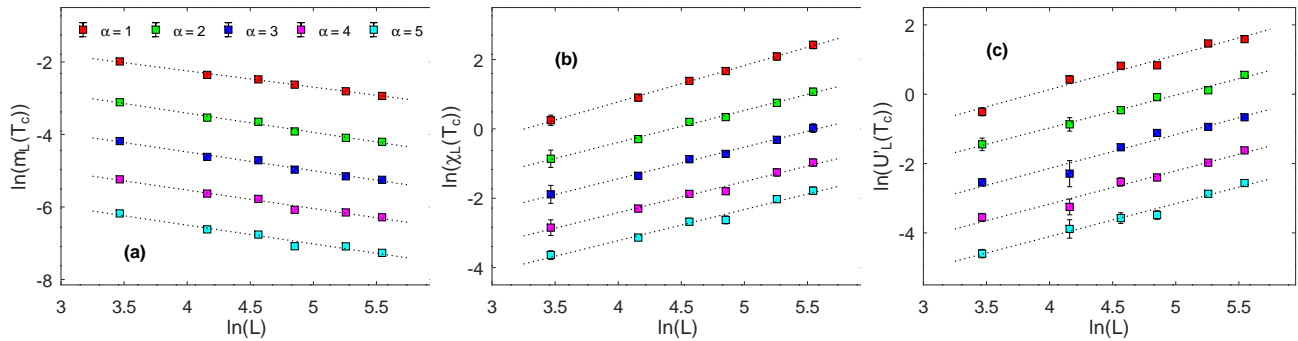


Figure 6. Log-log plots of (a) the magnetization  $m_L$ , (b) the susceptibility  $\chi_L$ , and (c) the derivative of the cumulant  $U'_L$ , at the critical point, as a function of the effective length  $L$ . We have fixed the values of  $k_0 = 4$ ,  $k_m = 10$ , and some selected values  $\alpha$ , as indicated in the figure. As we are interest is only on the slope, the linear coefficients are changed for better visualization of each of the curves. The slopes obtained here can be seen in Tab. I.

$\alpha$	$T_c$	$\beta$	$\gamma$	$\nu_{m_L}$	$\nu_{\chi_L}$
1	$6.228 \pm 0.004$	$0.47 \pm 0.03$	$1.03 \pm 0.03$	$1.00 \pm 0.06$	$1.00 \pm 0.04$
2	$5.734 \pm 0.008$	$0.55 \pm 0.02$	$0.95 \pm 0.03$	$1.03 \pm 0.03$	$1.05 \pm 0.04$
3	$5.225 \pm 0.009$	$0.57 \pm 0.03$	$0.91 \pm 0.05$	$0.96 \pm 0.05$	$1.08 \pm 0.03$
4	$4.710 \pm 0.020$	$0.56 \pm 0.03$	$0.90 \pm 0.04$	$1.05 \pm 0.05$	$1.10 \pm 0.03$
5	$4.210 \pm 0.020$	$0.58 \pm 0.03$	$0.92 \pm 0.05$	$1.03 \pm 0.04$	$1.10 \pm 0.05$

Table II. As a function of  $\alpha$ , here is showed critical temperature  $T_c$  present in the phases diagram of Fig. 5, and critical exponents obtained by the data collapse method, being that  $\nu_{m_L}$  and  $\nu_{\chi_L}$  are the correlation length exponent obtained by the magnetic and magnetic susceptibility data collapsed curves, respectively.

in  $\alpha = 5$ , and  $\beta = 1/(\alpha - 3)$ , and for  $3 < \alpha < 5$ . Interestingly, magnetic susceptibility critical exponent,  $\gamma$ , has a mean-field universal character for  $\alpha > 3$ , i.e.,  $\gamma = 1$  for the whole values of the exponents of the degree distribution in which a finite order phase transition is predicted,  $\langle k^2 \rangle < \infty$ . And in accordance with the scaling law relation  $\gamma/\nu = 2 - \eta$ , is also expected a universal mean-field character for correlation length,  $\nu = 1/2$ , and Fisher exponent,  $\eta = 0$  [24]. With this results, here, only for  $1 \leq \alpha \leq 5$  by limitation of the network size and computational time, we have made a direct comparative with this analytical results, using our *restricted* SFN. Therefore, we have calculated the critical exponents for the system, and this was made by two methods. One of these methods, using the FSS relations, is based on the slope of its linear fit, with the thermodynamic quantities near to critical point, and the second one, is based on the data collapse of thermodynamic quantities in the form of scaling functions [18–20].

We can find the critical exponents of the system by using two methods. In the first method, we have used the data of thermodynamic quantities near the critical point and for different network sizes. For instance, in a log-log plot in Fig. 6, we have fitted the thermodynamic quantities as a function of the effective length of the system  $L$  and its slope returns us the ratios between the critical exponents present in Eqs. (6), (7) and (8). For the ratio  $-\beta/\nu$  present in Eq. (6), the curves of magnetization for different network sizes and values  $\alpha$  is presented in Fig. 6(a), where we shown its linear fits. In the same way, but now for the ratio  $\gamma/\nu$ , using the Eq. (7), the linear fit of magnetic susceptibility curves can be seen in Fig. 6(b). Only these two ratios does not give us all the critical exponents of the system. Therefore, we also have used the forth-order Binder cumulant curves and its derivative, Eq. (8), being that its linear fits is presented in Fig. 6(c), and give us the ratio  $1/\nu$  that is the inverse of correlation length exponent, and only then obtain the exponents  $\beta$  and  $\gamma$ . The set of exponents obtained by this method can be found in Tab. I. However, it is necessary to emphasize that, because we are dealing with a random network with modifiable degree distribution, it is required to modify the Eqs. (6), (7) and (8) to the mean-field scaling relations, in which we change the effective length  $L$  by the total number of spins on network,  $N$ . This modification in the scaling relations can be easily implemented in the obtained critical exponents, dividing  $\nu$  by two, once that  $N = L^2$ .

In the second method, we can improve the values found for the critical exponents, by collapsing the data points. Our main goal is to use the thermodynamic quantities curves and different network sizes to obtain the form of its scaling functions, as a function of  $L^{1/\nu}\epsilon$ . It is possible because, in the proximity of the critical points, scaling functions in Eqs. (6), (7) and (8) must be independently of network sizes, if on its, is utilized the correct critical exponents of the system, i.e., in the proximity of  $T_c$  using the correct exponents on scaling relations we obtain a collapsed curve in the form of scaling functions. In Fig. 7, we show some examples of the best collapsed curves obtained. In this figure,

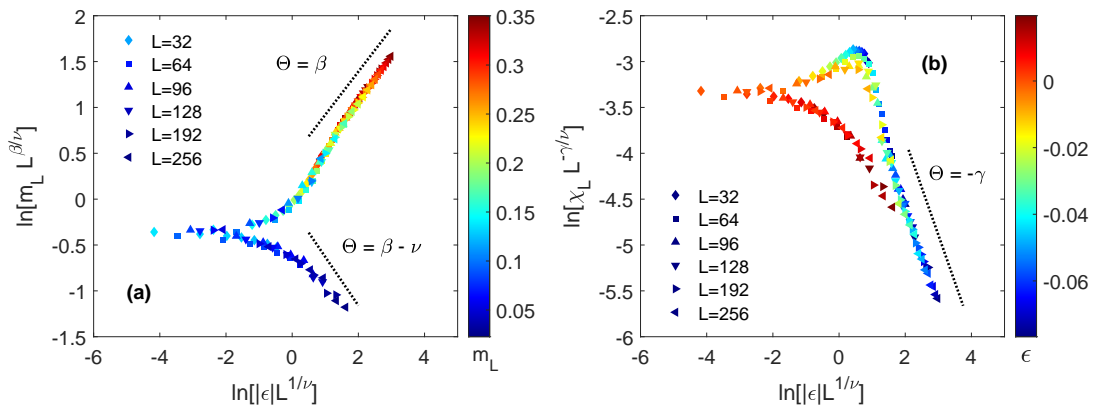


Figure 7. Data collapse near the critical point for the magnetization  $m_L$  (a) and susceptibility  $\chi_L$  (b) for different network sizes, as shown in the figure. Here, the minimum and maximum degree are fixed  $k_0 = 4$ ,  $k_m = 10$ , and  $\alpha = 1$ . The log-log plots were used to obtain the slope  $\Theta$  of scaling functions asymptotic behavior, i.e., distant of  $\epsilon = 0$ . The straight-dashed lines represent the asymptotic behavior of the scaling functions, Eq. (6) and (7).

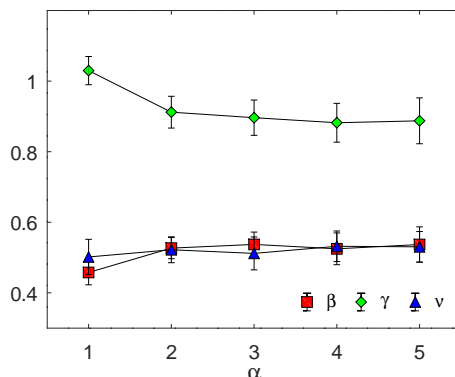


Figure 8. Static critical exponents  $\beta$ ,  $\gamma$ , and  $\nu$  as functions of the exponent  $\alpha$ .

what we have done is adjust the exponents on isolated scaling functions,  $m_0$  and  $\chi_0$ , as a function of  $L^{1/\nu}\epsilon$ , and when the thermodynamic quantity with different network size, best collapses into a single curve, that exponents were considered the critical exponents of the system. Fig. 7(a) shown, for  $\alpha = 1$ , the collapsed curves of magnetization data, Eq. (6), in which allowed us to adjust and obtain the exponents  $\beta$  and  $\nu$ , and besides that, in Fig. 7(b) also for  $\alpha = 1$ , magnetic susceptibility data, Eq. (7), enable us to obtain exponents  $\gamma$  and  $\nu$ . That estimated critical exponents for  $1 \leq \alpha \leq 5$  is presented in Tab. II, but, we also have to take into account the modification in scaling functions for the mean-field character, and the real values of exponent  $\nu$ , is only obtained dividing its results by two.

To the best comprehension of the critical exponents obtained for the *restricted* SFN, the average of its values, which is equivalent in both methods utilized in this work, was plotted in Fig. 8 as a function of  $\alpha$ . In lower values of  $\alpha$ , we tend to a system with all the degrees having the same number of sites and the mean-field critical behavior is present, but, when  $\alpha$  increase, the number of more connected sites decreases, and a slight deviation from this behavior is observed. With that observations, we can say that degree-degree correlations, also causes a deviation from the expected mean-field behavior on random networks with degree distribution convergent moments [24–26].

## V. CONCLUSIONS

Here, we have employed Monte Carlo simulations to the study of thermodynamic quantities and the critical behavior of the Ising model on a *restricted* SFN. When we fix the maximum  $k_m$  and minimum  $k_0$  number of degrees for the whole network sizes, as we made on our *restricted* SFN, we always have convergent moments based in the degree distribution  $P(k)$ . We have used a power-law degree distribution, and as the analytical results predict, the convergent second and fourth moments in the arbitrary degree distributions present a finite order phase transition [12, 13, 17, 24]. We have obtained the critical points of second-order phase transitions and built phase diagram of temperature  $T$  as



a function of  $k_0$  and  $k_m$ , and in which when we have  $k_0 = k_m$  a random uncorrelated network is obtained. Therefore, the critical points are in agreement with analytical calculations, but, the increase on difference between  $k_0$  and  $k_m$ , also increase the degree-degree correlations and causes a deviation from that calculations. The phase diagram of temperature  $T$  as a function of  $\alpha$  also was built, where we always have a finite critical temperature and a decrease in the critical point as we increase  $\alpha$ , once that we also decrease the number of more connected sites on network. With these critical points, we estimated the critical exponents for the system as a function of  $\alpha$ , and different from what is predicted by analytical results in a random uncorrelated SFN, here, with lower values of  $\alpha$ , the increase in the number of more connected sites reaches a mean-field critical behavior. Otherwise, when  $\alpha$  increase, a mean-field critical behavior is also observed, but how are we dealing with correlated degrees on network, the decreasing in the number of more connected sites causes a slight deviation on that exponents. That mean-field behavior was predicted on networks with convergent moments on its degree distribution and it was found on a diversity of complex networks [24–26]. In our work, it was made on the Ising model with a power-law degree distributed network and unexpected values of  $\alpha$ .

- 
- [1] R. Albert and A.-L. Barabási. *Rev. Mod. Phys.*, 74, 47 (2002);
  - [2] A.-L. Barabási. *Network Science*, (Cambridge University Press, NewYork, EUA, 2016);
  - [3] A.-L. Barabási and R. Albert. *Science*, 286, 509 (1999);
  - [4] M. Krasnytska, B. Berche, Y. Holovatch and R. Kenna. *Entropy*, 23, 1175 (2021);
  - [5] D.-H. Kim, G. J. Rodgers, B. Kahng and D. Kim. *Phys. Rev. E*, 71, 056115 (2005);
  - [6] S. N. Dorogovtsev, A. V. Goltsev and J. F. F. Mendes. *Eur. Phys. J. B*, 38, 177 (2004);
  - [7] G. Bianconi and A.-L. Barabási. *Phys. Rev. Lett.*, 86, 5632 (2001);
  - [8] C. P. Herrero. *Phys. Rev. E*, 91, 052812 (2015);
  - [9] S. Aparicio, J. Villazón-Terrazas and G. Álvarez. *Entropy*, 17, 5848 (2015);
  - [10] A. L. M. Vilela, B. J. Zubillaga, C. Wang, M. Wang, R. Du and H. E. Stanley. *Sci. Rep.*, 10, 8255 (2020);
  - [11] T. Gradowski and A. Krawiecki. *A. Phys. Pol. A*, 127, 1540 (2015);
  - [12] S. N. Dorogovtsev, A. V. Goltsev and J. F. F. Mendes. *Phys. Rev. E*, 66, 016104 (2002);
  - [13] A. V. Goltsev, S. N. Dorogovtsev and J. F. F. Mendes. *Phys. Rev. E*, 67, 026123 (2003);
  - [14] A. Aleksiejuk, J. A. Holyst and D. Stauffer. *Physica A*, 310, 260 (2002);
  - [15] G. Bianconi. *Phys. Lett. A*, 303, 166 (2002);
  - [16] C. P. Herrero. *Phys. Rev. E*, 69, 067109 (2004);
  - [17] M. Leone, A. Vazquez, A. Vespignani and R. Zecchina. *Eur. Phys. J. B*, 28, 191 (2002);
  - [18] K. Binder and D. W. Heermann. *Monte Carlo Simulation in Statistical Physics*. An Introduction, 6rd ed. (Springer, Cham, Switzerland, 2019);
  - [19] K. Binder and D. P. Landau. *A Guide to Monte Carlo Simulations in Statistical Physics*, 4rd ed. (TJ International Ltd, Padstow, UK, 2015);
  - [20] L. Böttcher and H. J. Herrmann. *Computational Statistical Physics*, 1rd ed. (Cambridge University Press, NewYork, EUA, 2021);
  - [21] S.-H. Tsai and S. R. Salinas. *Braz. J. Phys.*, 28, 1, (1998);
  - [22] M. E. J. Newman. *Phys. Rev. Lett.*, 89, 208701 (2002);
  - [23] M. Catanzaro, M. Boguña and R. Pastor-Satorras. *Phys. Rev. E*, 71, 027103 (2005);
  - [24] S. N. Dorogovtsev, A. V. Goltsev and J. F. F. Mendes. *Rev. Mod. Phys.*, 80, 1275 (2008);
  - [25] R. A. Dumer and M. Godoy. *Eur. Phys. J. B* 95, 159 (2022);
  - [26] A. Barrat and M. Weigt. *Eur. Phys. J. B*, 13, 547 (2000).